VERTICAL-VELOCITY SKEWNESS
IN THE MARINE STRATUS-TOPPED BOUNDARY LAYER

Chin-Hoh Moeng, Richard Rotunno, and Ilga Paluch
National Center for Atmospheric Research*
P.O. Box 3000, Boulder, Colorado

1. Motivations

Vertical-velocity skewness, $S_w \equiv \overline{w^3}/(\overline{w^2})^{3/2}$, in a turbulent flow is important in several regards. S_w is indicative of the structure of the motion—when it is positive, updrafts are narrower and stronger than surrounding downdrafts, and vice versa. The quantity $\overline{w^3}$ represents the vertical flux of the vertical component of turbulence energy, which dominates the turbulent energy transport in buoyancy-driven turbulence. Therefore, $\overline{w^3}$ may be an important quantity that determines the entrainment rate in the buoyancy-driven boundary layer.

Aircraft measurements often suggest cool, narrow downdrafts at some distance below the stratus cloud top, indicating a negative S_w (Nicholls and Leighton, 1986). This seems natural as the turbulence within the stratus-topped boundary layer (CTBL) is driven mainly by the radiative cooling at the cloud top (although sometimes surface heating can also play a major role.) One expects intuitively (e.g., Nicholls, 1984) that, in the situations where cloud-top cooling and surface heating coexist, the turbulence statistics in the upper part of the CTBL are influenced more by the cloud-top cooling, while those in the lower part, more by the surface heating. Thus one expects negative S_w in the upper part, and positive in the lower part, in this case. In contradistinction, large-eddy simulations (LES) of the CTBL show just the opposite: The S_w is *positive* in the upper part and *negative* in the lower part of the layer. Figure 1 shows the vertical distribution of $\overline{w^3}$ and S_w from a $(40)^3$ large-eddy simulation (Moeng, 1986) of the CTBL with both cloud-top cooling and surface heating.

To understand the nature of vertical-velocity skewness, we study the simplest type of buoyancy-driven turbulence—turbulent Rayleigh-Benard convection—through direct numerical simulations. The following is an abstract version of the paper by Moeng and Rotunno (1989).

2. Turbulent Rayleigh-Benard convections

Consider a shallow, incompressible fluid between two infinite horizontal plates with the bottom one maintained at a higher temperature than the top. When the Rayleigh number, $R_a \equiv g\beta\Delta T D^3/(\mu\kappa)$, is larger than a critical number, the fluid is unstable and if large enough becomes turbulent. Here, D is the distance between the upper and lower plates,

ΔT is the temperature difference between the plates, g is the acceleration of gravity, β is the coefficient of volume expansion, and μ and κ are the coefficients of molecular viscosity and conductivity.

1.5

(a)

(b)

1.0

z/z_i

Cloud
Layer

0.5

0

-0.2   -0.1   0   0.1   0.2 -1.0 -0.5   0   0.5   1.0

$$\overline{w^3}/w_*^3 \qquad \overline{w^3}/\overline{w^2}^{3/2}$$
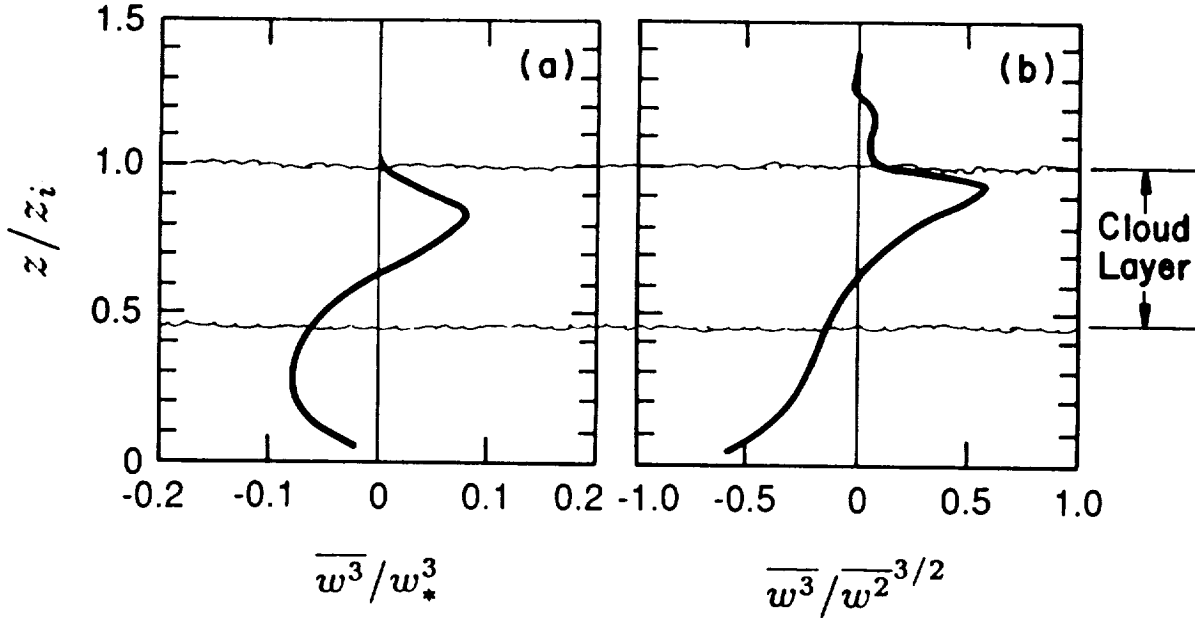
Figure 1 Profiles of (a) flux of vertical-velocity variance, and (b) vertical-velocity skewness in the stratus-topped boundary layer obtained in a $(40)^3$ large-eddy simulation (after Moeng 1986.) The convective scaling velocity, $w_* \equiv [\beta g z_i B_c]^{1/3}$, where B_c is the layer-averaged buoyancy flux in the cloud layer.

Direct numerical simulations solve the Navier-Stokes equations exactly with no uncertain parameters, thus the simulations are in a sense exact except possible numerical errors. We carry out two experiments in the fully turbulent regime (at R_a on the order of 10^5): Experiment HC (for 'Heating and Cooling') includes both bottom heating and top cooling. Experiment H (for 'Heating') has only bottom heating. Although we do not actually carry out an Experiment C (for 'Cooling'), we will refer to it as such with the understanding that it is a symmetry of Experiment H with obvious sign changes on the w and T fluctuations.

Figure 2 shows S_w-distributions for Experiments H, C, and HC. Bottom-heating-only generates positive vertical-velocity skewness throughout and S_w increases with height alway from the source. Similarly, top-cooling-only generates negative vertical-velocity skewness throughout and its negative magnitude increases downward away from the source. When bottom heating and top cooling coexist, S_w is positive in the upper layer and negative in the lower layer. Adding S_w-distribution from Experiment H to that from Experiment C, we obtain a profile similar to that from Experiment HC.

Therefore, understanding the nature of the S_w-distribution for the bottom-heating-

only (or the top-cooling-only) is necessary first step toward understanding why there is negative S_w in the lower half and positive S_w in the upper half in the case with both top-cooling and bottom-heating.
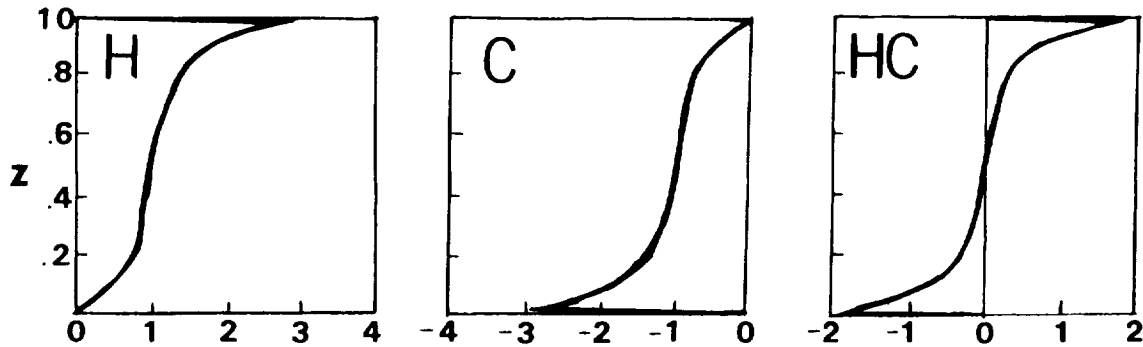

Figure 2 Profiles of vertical-velocity skewness from Experiments H, C, and HC.

3. Physical mechanism responsible for w-skewness

The mechanism responsible for the increase of S_w with height in the bottom-heating case can be easily understood by examining the structure of the turbulent eddies. The planform structure shown in Fig. 3 indicates an irregular cellular pattern in the lower levels, and more isolated and discrete updrafts in the upper levels. The total area covered by updrafts decreases with height. Since the skewness is related to the ratio of the total area covered by updrafts to the area covered by downdrafts, Fig. 3 indicates an increase of S_w with height.
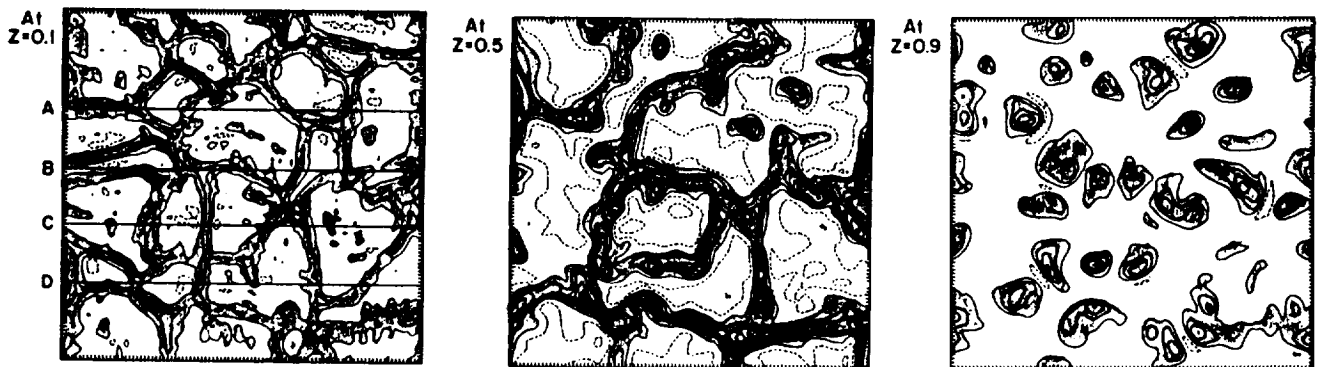

Figure 3 Horizontal cross sections of w from Experiment H. The shaded areas indicate positive values. The solid and dashed contour lines (contour interval, 0.1) represent positive and negative values, respectively. Vertical cross sections through the locations marked A,B,C and D are shown in Fig. 4.

To get a better view of the eddy structure, we show in Fig. 4 the vertical cross sections along four y-locations marked in the left panel of Fig. 3. Here we see a few big eddies penetrate into the top, while others never make it to the top, which is typical for a fully developed turbulent flow. The area covered by individual updrafts remains relative constant with height, while the number of updrafts decreases. Therefore, the net area covered by updrafts decreases with height, and S_w increases with height.
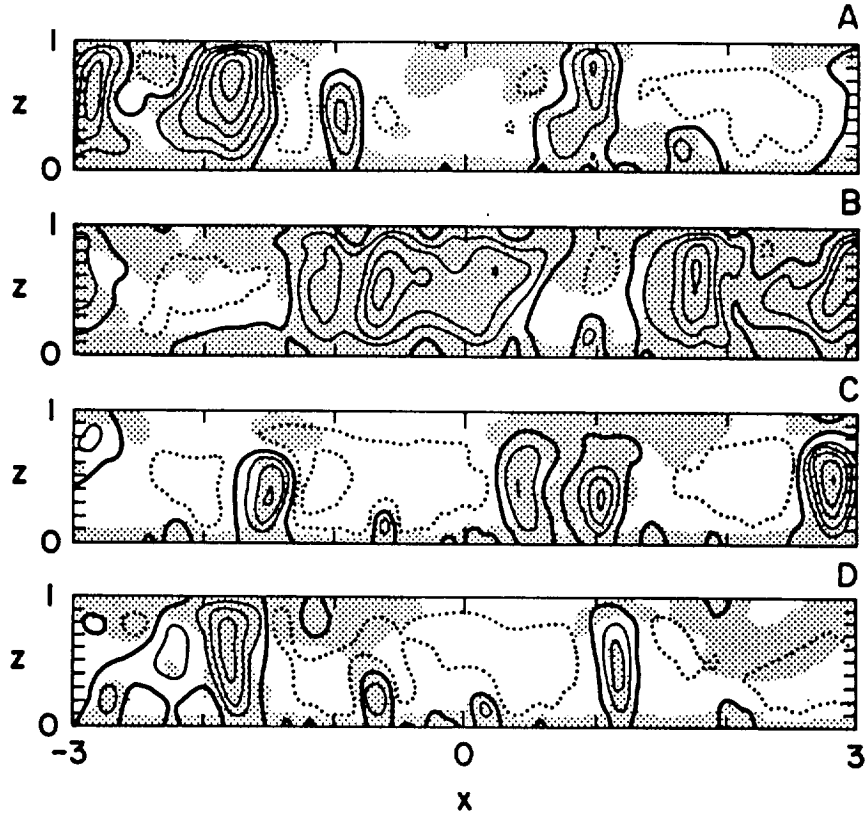

Figure 4 Vertical (x-z) cross sections through the locations marked in Fig. 3. The shaded area represents regions where $T - \overline{T} > 0.3$. Areas of $w > 0$ are enclosed by the thick solid line; the solid and dotted contour lines (contour interval, 0.1) indicate positive and negative values of w, respectively.

4. Stratus-topped PBL

When a stratus cloud layer exists in the upper part of the PBL, there is always longwave radiative cooling at the cloud top. For the case of no surface buoyancy flux, the CTBL resembles Experiment C, and for the case with a positive surface flux, it resembles Experiment HC, except for the difference of existing entrainment process in the CTBL.

In the case with a positive surface flux, the LES results show negative S_w in the lower

half and positive S_w in the upper half of the CTBL, in agreement with Experiment HC. Nicholls and Leighton (1986)'s aircraft data show negative S_w within some distance below cloud top (their Fig. 12). With only one exception, the cases they analyze have zero surface fluxes. Therefore S_w should be negative throughout the CTBL, as indicated by Experiment C, and it is so observed.

We have analyzed the FIRE data for S_w. We will present our results in the meeting.

REFERENCES

Moeng, C.-H., 1986: Large-eddy simulation of a stratus-topped boundary layer. part I: Structure and budgets. *J. Atmos. Sci.*, **43**, 2886–2900.

Moeng, C.-H. and R. Rotunno, 1989: Vertical-velocity skewness in the buoyancy-driven boundary layer. Submitted to *J. Atmos. Sci.*

Nicholls, S., 1984: The dynamics of stratocumulus: aircraft observations and comparisons with a mixed-layer model. *Quart. J. Roy. Meteorol. Soc.*, **110**, 783–820.

Nicholls, S. and J. Leighton, 1986: An observational study of the structure of stratiform cloud sheets: Part I. Structure. *Quart. J. Roy. Meteorol. Soc.*, **112**, 431–460.